SIAM J. SCI. COMPUT.
Vol. 21, No. 1, pp. 255–282




# ABSORBING BOUNDARY CONDITIONS FOR THE SCHRÖDINGER EQUATION*

THOMAS FEVENS† AND HONG JIANG‡

**Abstract.** A large number of differential equation problems which admit traveling waves are usually defined on very large or infinite domains. To numerically solve these problems on smaller subdomains of the original domain, artificial boundary conditions must be defined for these subdomains. One type of artificial boundary condition which can minimize the size of such subdomains is the absorbing boundary condition. The imposition of absorbing boundary conditions is a technique used to reduce the necessary spatial domain when numerically solving partial differential equations that admit traveling waves. Such absorbing boundary conditions have been extensively studied in the context of hyperbolic wave equations. In this paper, general absorbing boundary conditions will be developed for the Schrödinger equation with one spatial dimension, using group velocity considerations. Previously published absorbing boundary conditions will be shown to reduce to special cases of this absorbing boundary condition. The well-posedness of the initial boundary value problem of the absorbing boundary condition, coupled to the interior Schrödinger equation, will also be discussed. Extension of the general absorbing boundary condition to higher spatial dimensions will be demonstrated. Numerical simulations using initial single Gaussian, double Gaussian, and a narrow Gaussian pulse distributions will be given, with comparision to exact solutions, to demonstrate the reflectivity properties of various orders of the absorbing boundary condition.

**Key words.** Schrödinger equation, absorbing boundary conditions, radiation boundary conditions, initial-boundary value problems

**AMS subject classifications.** 35L35, 65M99, 35A40

**PII.** S1064827594277053

## 1. Introduction.

A large variety of numerical calculations involving the solutions to partial differential equations requires the imposition of artificial boundary conditions to delimit the computational domain to a manageable size. This often happens when the natural domain for the problem being solved is infinite and thus the natural boundary conditions for the problem are defined at infinity. But if we desire the numerical solution on only a finite section of the domain, the use of artificial boundary conditions is necessitated. It is a requirement of such artificial boundary conditions not to adversely affect the numerical calculation in the interior domain. Specifically, we will consider problems where traveling waves are present.

If standard Dirichlet or Neumann boundary conditions are used for our artificial boundary conditions, then in many cases a traveling wave evolved via a wave equation will view the boundary condition as an impenetrable barrier and the wave would be completely reflected back into the interior domain. Obviously, this type of boundary condition would not serve our purposes since the reflected wave would disrupt the interior solution. The only way that such a boundary condition could be used would be to place the boundary condition at a large distance from the relevant interior solution, such that the reflected wave would not affect the interior solution until

*Received by the editors November 9, 1994; accepted for publication (in revised form) May 18, 1998; published electronically Semptember 1, 1999.

http://www.siam.org/journals/sisc/21-1/27705.html

†Department of Computing and Information Science, Queen's University, Kingston, Ontario, K7L 3N6, Canada (fevens@qucis.queensu.ca). The research of this author was supported in part by an Information Technology Research Centre bursary.

‡Bell Labs, Lucent Technologies, Murray Hill, NJ 07974-0636 (hjiang@emailbox.hdtv.lucent.com). The research of this author was supported in part by the Natural Sciences and Engineering Research Council of Canada.

a large number of time steps (before which the solution would be obtained). This approach would be costly for multidimensional problems or problems evolving over many time steps. It would be preferable to use artificial boundary conditions which do not affect the interior solution but which don't have to be placed at a large distance from the relevant interior solution.

Since the boundary condition must be coupled with the interior solution, the boundary condition must be well-posed with respect to the interior solution, and the boundary condition must be stable such that the numerical solution will remain bounded. Also, the artificial boundary condition should annihilate all incident waves so as to produce no reflections which would then propagate into the interior domain. Boundary conditions which satisfy all these conditions are called absorbing (or open, radiation, or transparent) boundary conditions. The use of absorbing boundary conditions allows for the numerical solution of problems involving traveling waves with a minimal number of spatial points while maintaining the accuracy desired for the solution. This can result in problems being solved more quickly and can allow for the solution of more complex problems, especially in higher dimensions.

In this paper, we will review the relevant previous work that has been done with respect to absorbing boundary conditions for wave equations and similar differential equations. Then we will introduce the Schrödinger equation for which we will develop absorbing boundary conditions. We will discuss previously considered absorbing boundary conditions for the Schrödinger equation and then derive a new absorbing boundary condition. We will show that the previously published absorbing boundary conditions for the Schrödinger equation reduce to special cases of the new absorbing boundary condition. We will then consider the well-posedness properties of the initial boundary value problem of the Schrödinger equation coupled to the absorbing boundary condition. Also, we will outline how our general absorbing boundary condition can be extended to higher dimensional problems. Finally, we will use a finite-difference scheme to solve the Schrödinger equation, and we will consider the properties of several numerical simulations using various orders of the absorbing boundary condition.

**2. Review of absorbing boundary conditions.** In this section, we will consider previous work that has been done to devise absorbing boundary conditions for various wave equations. Absorbing boundary conditions may be divided into boundary conditions for dispersive or nondispersive equations. A dispersive equation is one that admits plane wave solutions of the form $\mathrm{e}^{-i(\omega t-kx)}$ and in which the speed of propagation of the wave is partially, or completely, a function of the wave number $k$. For solutions for a given wave equation, $\omega$ is a function of $k$ and is called the *dispersion relation* for the differential equation. The dispersion relation allows us to define the phase speed, $c(k) = \frac{\omega(k)}{k}$, of individual waves and the group velocity, $C(k) = \frac{d\omega}{dk}(k)$, of wave packets. Energy, for instance, travels with group velocity. Although a differential equation may be nondispersive (for example, the scalar wave equation), its discretization will nearly always be dispersive [24], so we will consider only dispersive equations. We will review work that has been done to devise absorbing boundary conditions for particular differential equations, exploiting these and other properties of dispersive equations.

**2.1. Absorbing boundary conditions for wave equations.** A fundamental requirement of an absorbing boundary condition is that the interior solution that is generated is close to the unique solution that is produced if the boundary conditions

were placed at a large distance (say, infinity) from the interior region. For interior schemes involving traveling waves, the absorbing boundary condition must have the ability to absorb waves incident on it rather than reflecting them back into the interior of the domain.

**2.1.1. Engquist and Majda approach.** In their paper [2], Engquist and Majda proposed a pseudodifferential operator which acts as a perfectly absorbing boundary condition for the scalar wave equation

$$\frac{\partial^2 u}{\partial t^2} - \frac{\partial^2 u}{\partial x^2} - \frac{\partial^2 u}{\partial y^2} = 0 \tag{2.1}$$

with the related dispersion relation

$$\omega^2 = k^2 + l^2. \tag{2.2}$$

The exact absorbing boundary condition is obtained by inverting this dispersion relation to get an expression for $k$:

$$k = \pm\sqrt{\omega^2 - l^2} = \pm\omega\sqrt{1 - l^2/\omega^2}. \tag{2.3}$$

If the positive branch of this equation is chosen and a mapping is made between the dual of a variable and its related differential operator (via a Fourier transform which involves integrating over all possible values of the duals), the result is a pseudodifferential equation which applied to the $x = L$ boundary which would perfectly absorb all right-traveling waves impinging on the boundary. However, since the pseudodifferential form of the absorbing boundary condition is nonlocal and thus not directly implementable in a finite-different scheme, Engquist and Majda derive local approximations to (2.3) by expanding out the square root into terms of the Padé series to various orders of accuracy. A hierarchy of local absorbing boundary conditions may be derived using higher order approximations. In a second paper, Engquist and Majda introduce a two-dimensional version of their approximations based on an expression in the angle of the wave measured with respect to the normal of the boundary [3].

**2.1.2. Canonical absorbing boundary conditions.** Higdon showed that the higher order approximations to (2.3) with their accompanying substitutions of corresponding differential operators ($i\omega \to \frac{\partial}{\partial t}$, etc.) may be expressed in the following canonical form [9], [11]:

$$\left[\prod_{j=1}^{p}\left(\frac{\partial}{\partial x} - (\cos\alpha_j)\frac{\partial}{\partial t}\right)\right] u|_{x=0} = 0. \tag{2.4}$$

This canonical form reduces to Engquist and Majda's boundary conditions, based on Padé approximations, when $\alpha_j = 0$. Boundary conditions of this form were also derived independently by Keys [15]. Higdon was able to generalize Engquist and Majda's approximations of the exact absorbing boundary condition (2.3) in two important ways. First, he showed that Engquist and Majda's approximations could be factorized into first order differential operators, similar to

$$\left(\frac{\partial}{\partial x} - \frac{\partial}{\partial t}\right) u|_{x=0} = 0. \tag{2.5}$$

Furthermore, he generalized the factors such that they would annihilate waves incident on the boundary at any angle, rather than optimally at the normal. This more general form greatly simplifies implementation and stability analysis.

Another approach, using group velocity, to derive absorbing boundary conditions was proposed by Jiang and Wong [14]. Their global absorbing boundary condition applies to any linear hyperbolic equation with constant coefficients where the dispersion relation is known (for example, the wave equation or the Klein–Gordon equation). Jiang and Wong's approach considers the group velocity, $C(k)$, of the solution at the boundaries. Remember that the flow of energy propagates at the group velocity. If we consider the $x = 0$ boundary, any component of the solution which has a positive group velocity would obviously be a component of a reflected wave. Therefore, a boundary condition which does not admit reflected waves can be expressed in the following manner:

$$C(k)|_{x=0} = -\left|C(k)|_{x=0}\right|. \tag{2.6}$$

Unfortunately, like Engquist and Majda's perfectly absorbing boundary condition (2.3), this absorbing boundary condition, when mapped into differential form, is nonlocal, due to the absolute value function, and thus a rational approximation is necessary.

To do this, Jiang and Wong use an approach similar to that utilized by Higdon [9]. First, a first order approximation is developed from the exact boundary condition (2.6) by assuming that the incident wave has a certain group velocity, $b$, which is then absorbed at the $x = 0$ boundary by

$$C(k)|_{x=0} + b = 0. \tag{2.7}$$

Let us consider the wave equation (2.1) whose dispersion relation is given in (2.2). In this case,

$$C(k) = \frac{\partial \omega(k,l)}{\partial k} = \frac{k}{\omega}.$$

Therefore, boundary condition (2.7) is equivalent to the symbol $k + b\omega = 0$ or, remembering the corresponding differential operators,

$$\left(\frac{\partial}{\partial x} - b\frac{\partial}{\partial t}\right) u|_{x=0} = 0. \tag{2.8}$$

Therefore, taking Higdon's lead [9], the canonical form of this absorbing boundary condition is

$$\left[\prod_{j=0}^{p}\left(\frac{\partial}{\partial x} - b_j\frac{\partial}{\partial t}\right)\right] u|_{x=0} = 0. \tag{2.9}$$

This is equivalent to Higdon's canonical form if $b_j = \cos\alpha_j$. As before, (2.9) is perfectly absorbing for incident waves with group velocities $b_j$. The advantage of this approach is all we need is the dispersion relation, and we can derive the absorbing boundary conditions to any order by using the group velocity.

In [13], Higdon developed canonical radiation boundary conditions for the dispersive wave equation. Higdon showed that the performance of the boundary condition

was not sensitive to the choice of parameters for the boundary condition. Furthermore, Higdon showed that another absorbing boundary condition developed for the dispersive wave would be equivalent to his canonical form, unstable, or not optimal in the sense that the absorbing boundary condition could be modified, without increasing its order, to make it more effective. Thus, if a canonical absorbing boundary condition is found, through using phase velocity, group velocity, or another technique, it will reduce to one ideal canonical form.

For references to other work in development of absorbing boundary conditions, see [4].

**2.2. Stability and well-posedness of absorbing boundary conditions.** Of course, if a boundary condition is unstable or generates spurious solutions, it is flawed. Issues related to stability and well-posedness of absorbing boundary conditions have been considered by a number of researchers.

The main theoretical work describing the well-posedness of initial boundary value problems has been done by Kreiss [17], Sakamoto [22], and others. The well-posedness of absorbing boundary conditions for the wave equation in particular has been considered by Trefethen and Halpern [26]. The well-posedness properties of particular absorbing boundary conditions are considered in [1], [2], [10], [12], [14], [21] by their authors.

The well-posedness theory is closely related to the stability of finite-difference approximations of initial boundary value problems for hyperbolic equations. The stability criterion for hyperbolic initial boundary value problems is outlined by Gustafsson, Kreiss, and Sundström [7], with a group velocity interpretation of their rather abstract criterion given by Trefethen [25]. Higdon considers the theory related to well-posedness of initial boundary value problems for linear first order hyperbolic systems [10].

**3. New absorbing boundary conditions.** In this Section, we will develop flexible absorbing boundary conditions for the Schrödinger equation.

**3.1. The Schrödinger equation.** The following is the one-dimensional Schrödinger equation:

$$i\hbar\frac{\partial\Psi}{\partial t}(x,t) = -\frac{\hbar^2}{2m}\frac{\partial^2\Psi}{\partial x^2}(x,t) + V\Psi(x,t). \tag{3.1}$$

If $V$ is a constant, or if it is a slowly varying function of $x$ and $t$, then the dispersion relation is given by

$$\hbar^2k^2 = 2m\left[\omega\hbar - V\right], \tag{3.2}$$

where $m$ is the mass of the particle, $V$ is the potential, $\Psi$ is the wave-function, $\hbar = h/2\pi$ where $h$ is Planck's constant, and $i = \sqrt{-1}$. The Schrödinger equation is a fundamental equation in the field of quantum physics. It is used to describe the propagation of a quantum particle, such as an electron, in a potential background described by $V$. If $V = 0$, then the particle is moving in a vacuum. The square of the wave-function, $|\Psi|^2$, describes the probability distribution for the position of the particle.

**3.2. Previous absorbing boundary conditions.** Several techniques have been considered for boundary conditions which would remove spurious reflections from artificial boundaries during the numerical solution of the one-dimensional Schrödinger

equation. Kosloff and Kosloff [16] used an enlarged computational domain and then applied a damping (or penalty) function in the artificial part of the domain to decrease the amplitude of outgoing waves. Although this method can produce good results, the enlarged domain is costly, especially for extensions to higher dimensions. A related approach was considered by Neuhauser and Baer [20], where they added a negative complex short-range potential to the potential in the asymptotic region outside the computational domain to construct nearly perfect absorbing boundary conditions.

Work by Shibata [23] and Kuska [19], which is based primarily on the work of Engquist and Majda [2], [3], has led to one-way absorbing boundary conditions for the Schrödinger equation. Their approach is to invert (3.2) to obtain an expression for the sign and magnitude of the wave number,

$$\hbar k = \sqrt{2m[\hbar\omega - V]}, \tag{3.3}$$

where the positive value for the square root corresponds to waves traveling in an increasingly positive $x$ direction and eventually impinging on the right-hand boundary ($x = L$). To obtain the expression for waves traveling the opposite direction, simply substitute $k$ with $-k$. A boundary condition of the form (3.3) is an exact absorbing boundary condition similar to Engquist and Majda's boundary condition in (2.3). To see this, consider all waves incident on the $x = L$ boundary satisfying (3.3). Then there are no waves where $\hbar k = -\sqrt{2m[\hbar\omega - V]}$ at the boundary, and thus there are no left-traveling (hence reflected) waves. But due to the square root function, (3.3) cannot be implemented directly in physical space, but rather (3.3) must be put in rational differential form, and thus into a finite-difference form, to be implemented on the boundary.

In order to develop a differential equation to create a boundary condition transparent to waves leaving the domain, the right-hand side of (3.3) must be approximated by a rational expression. In terms of the one-dimensional Schrödinger equation, two rational expressions for the square root function have been considered in the literature. The first was developed by Shibata [23] and has the form

$$\hbar k = \frac{\sqrt{2m\alpha_2} - \sqrt{2m\alpha_1}}{\alpha_2 - \alpha_1}\,[\hbar\omega - V] + \frac{\alpha_2\sqrt{2m\alpha_1} - \alpha_1\sqrt{2m\alpha_2}}{\alpha_2 - \alpha_1}, \tag{3.4}$$

where $\alpha_1$ and $\alpha_2$ are adjustable parameters. Equation (3.4) is a straight line interpolation of (3.3), which intersects the dispersion relation at two points.

A second approximation to (3.3) was developed by Kuska [19] and has the form

$$\hbar k = \hbar k_0 \frac{1 + 3z}{3 + z}, \tag{3.5}$$

with $z = 2m(\hbar\omega - V)/\hbar^2 {k_0}^2$. His absorbing boundary condition is based on an expansion of (3.3) about the value $\hbar k_0$. Equation (3.5) is essentially an approximation to (3.3) which intersects the square root function at only one point. Compared to Shibata's approximation (3.4), (3.5) is a higher order approximation over the length of the dispersion relation but is limited by the single interpolation point and is thus less flexible.

These absorbing boundary conditions developed by Shibata and Kuska are limited either in order of effectiveness or in flexibility to absorb different energies of incident waves.

**3.3. New absorbing boundary condition.** Here, we will consider an alternate approach to that used by Shibata and Kuska. First, we will assume that the potential $V$ is constant, or a slowly varying function, in the vicinity of the boundaries. Therefore, from the dispersion relation, (3.3), we can calculate the group velocity:

$$C = \frac{\partial \omega}{\partial k} = \frac{\hbar k}{m}. \tag{3.6}$$

This gives the group velocity of a wave packet as it is evolved by the Schrödinger equation.

The following approach of using the group velocity to develop absorbing boundary conditions was first used by Jiang and Wong for hyperbolic differential equations [14]. For a wave traveling to the right within the domain and impinging on the $x = L$ boundary, the group velocity from (3.6) must be positive, since the energy of the wave propagates at group velocity. This implies that the energy associated with $k$ is leaving the interior domain. A negative group velocity would mean that energy is entering the interior domain and hence is a reflected wave.

Put in mathematical form, the symbol for the boundary condition has the following form at the $x = L$ boundary:

$$\frac{\hbar k}{m} = \left| \frac{\hbar k}{m} \right|. \tag{3.7}$$

For the $x = 0$ boundary, simply replace $k$ with $-k$. The pseudodifferential boundary condition that could be developed from this symbol is an exact absorbing boundary condition if satisfied on the boundary since all the group velocities on the boundary are positive (no spurious reflections off the boundary). But, like (3.3), this boundary condition cannot be realized in physical space by differential operators due to the absolute value function, and thus we must use an approximation to obtain an explicit rational differential form which can be applied on the boundary.

Since a single differential equation can absorb only waves of a certain group velocity, let us consider an approximation to (3.7) of the form of

$$\frac{\hbar k}{m} \equiv a \tag{3.8}$$

on the boundary, where $a$ is positive and real. Using the correspondence between the dual $k$ and the partial derivative in $x$, we obtain the following differential operator relation from (3.8):

$$\left( i \frac{\partial}{\partial x} + \frac{ma}{\hbar} \right) \Psi = 0. \tag{3.9}$$

If this differential equation is satisfied on the boundary, then waves traveling to the right with group velocity $a$ would be absorbed completely, leading to no reflections off the boundary from that component of the numerical solution for the wave.

But in general waves are composed of more than one component with different group velocities. Therefore, a generalization of the operator in (3.9) is

$$\prod_{l=1}^{p} \left( i \frac{\partial}{\partial x} + \frac{ma_l}{\hbar} \right) \Psi = 0. \tag{3.10}$$

Here, the group velocity values, $a_l$, are real. For traveling waves, $\hbar k$ is real; therefore $\hbar\omega \geq V$ from (3.3) and (3.6). For waves traveling to the left and impinging on the $x = 0$ boundary, $a_l$ would be substituted with $-a_l$ in (3.10). The motivation for this generalization comes from a similar generalization that was considered by Higdon [9] which was shown to correspond to the known absorbing boundary conditions developed by Engquist and Majda [2] and others for wave equations, as discussed previously.

If $a_k \neq a_l,\ k \neq l$, then the effect of the differential equation (3.10), when applied to the boundary, would be to completely absorb $p$ different components of the computed wave solution with $p$ different group velocities, each being absorbed to the first order. If $a_k = a_l,\ k \neq l$, then the effect of this differential equation, when applied to the boundary, would be to completely absorb the component of the computed wave solution with group velocity $a_j$ to the $p$th order. Each $ma_i/\hbar$ can be considered as an interpolation point of the dispersion relation at the value $k$ in (3.2). Therefore, in (3.10) the $ma_i/\hbar$ interpolates (3.2) at different values of $k$ with $p$ being the order of the interpolation. If all the group velocities $a_i$ are the same, then (3.10) is essentially a series expansion of (3.2) to the $p$th order about the point $ma_i/\hbar$.

**3.4. Comparison with previous work.** Equation (3.10) is a general absorbing boundary condition from which it is possible to derive the specific absorbing boundary conditions presented by Shibata and Kuska. To see this, first consider $p = 2$. Then (3.10) has the symbol (where we have replaced $i\partial/\partial x$ with $-k$)

$$\left(-k + \frac{ma_1}{\hbar}\right)\left(-k + \frac{ma_2}{\hbar}\right) = 0. \tag{3.11}$$

If we multiply out (3.11) and solve for $\hbar k$, then we obtain

$$\hbar k = \frac{2}{a_1 + a_2}(\hbar\omega - V) + \frac{ma_1a_2}{a_1 + a_2}. \tag{3.12}$$

Here we have used (3.2) to substitute for $k^2$. Note that (3.12) is symmetric in $a_j$'s. To obtain the equation for left-going waves, replace the left-hand side of (3.12) with $-\hbar k$. Shibata's relationship in (3.4) reduces to (3.12) via the following substitutions:

$$\alpha_1 = \frac{ma_1{}^2}{2} \quad \text{and} \quad \alpha_2 = \frac{ma_2{}^2}{2}.$$

Although Kuska states that $\alpha_1$ and $\alpha_2$ as used by Shibata are two "unphysical parameters" [19], we may attach meaning to them in that they are kinetic energy parameters, where the kinetic energy is propagating at group velocities $a_1$ and $a_2$.

Now, consider $p = 3$. Then (3.10) has the symbol

$$\left(-k + \frac{ma_1}{\hbar}\right)\left(-k + \frac{ma_2}{\hbar}\right)\left(-k + \frac{ma_3}{\hbar}\right) = 0, \tag{3.13}$$

where the same substitution for $i\partial/\partial x$ was used. Again, using (3.2) to substitute for $k^2$, this simplifies to the relation

$$\hbar k = \frac{2mh_1(\hbar\omega - V) + h_3}{2m(\hbar\omega - V) + h_2}, \tag{3.14}$$

where

$$h_1 = m\left(a_1 + a_2 + a_3\right),$$

$$h_2 = m^2 a_1 a_2 a_3 \left( \frac{1}{a_1} + \frac{1}{a_2} + \frac{1}{a_3} \right),$$
$$h_3 = m^3 a_1 a_2 a_3.$$

Again, to obtain the equation for left-going waves, multiply the right-hand side of (3.14) by $-1$. We may obtain Kuska's symbol for his absorbing boundary condition (3.5) by letting $a_1 = a_2 = a_3 = \frac{\hbar k_0}{m}$.

Therefore, Shibata's relationship for $\hbar k$ is equivalent to our second order ($p = 2$) absorbing boundary condition and Kuska's relationship for $\hbar k$ is equivalent to a special case of our third order ($p = 3$) boundary condition. Kuska's special case absorbing boundary condition (3.5) would be expected to work well if the incident wave on the boundary were composed homogeneously of only one $k_0$ component. This absorbing boundary condition would be expected to remove the $k_0$ component of the reflected wave to the third order. However, if the incident wave were composed of a number of different group velocity components, a more general absorbing boundary condition would be needed, which could be "tuned" to remove the dominant reflected wave components. Otherwise, the components of the wave composed of wave packets traveling with different group velocities other than that associated with $k_0$ would be reflected to a large degree. (This will be quantified in the next subsection on reflection.)

Considering that Kuska's absorbing boundary condition is simply the third order form of (3.10) with identical $a_i$'s, we can derive the fourth order absorbing boundary condition for comparison. Note that part of the motivation in the development of previous two absorbing boundary conditions was to develop a boundary condition which is first order in the boundary variable of interest, which is $x$ in this case, and possibly of higher order in the other spatial and temporal variables. Hence, we obtain a boundary condition which is a first order differential on the incident boundary in order to obtain an "interior-pointing" finite-difference scheme. Continuing this approach, let $p = 4$ in (3.10), replacing the partial derivative in $x$ with its corresponding wave vector

$$4m^2(\hbar\omega - V)^2 + 2m(-g_1\hbar k + g_2)(\hbar\omega - V) - g_3\hbar k + g_4 = 0, \tag{3.15}$$

where

$$g_1 = m\left(a_1 + a_2 + a_3 + a_4\right),$$
$$g_2 = m^2\left(a_1a_2 + a_1a_3 + a_1a_4 + a_2a_3 + a_2a_4 + a_3a_4\right),$$
$$g_3 = m^3 a_1a_2a_3a_4\left(\frac{1}{a_1} + \frac{1}{a_2} + \frac{1}{a_3} + \frac{1}{a_4}\right),$$
$$g_4 = m^4 a_1a_2a_3a_4.$$

Again, we have replaced $k^2$ with its lower order equivalent from (3.2). If we let all the interpolation points be identical, $a_1 = a_2 = a_3 = a_4 = \frac{\hbar k_0}{m}$, then we obtain

$$\hbar k = \frac{\hbar k_0}{4}\left[\frac{z^2 + 6z + 1}{z + 1}\right], \tag{3.16}$$

where $z = 2m(\hbar\omega - V)/\hbar^2 k_0^2$. This would be the $p = 4$ absorbing boundary condition extension to Kuska's absorbing boundary condition.

**3.5. Reflection coefficients.** We can calculate an expression for the amount of reflection we can expect off the absorbing boundary condition (3.10). Consider a wave impinging on the $x = L$ boundary, with a reflected component:

$$\Psi = e^{-i(\omega t - kx)} + re^{-i(\omega t + kx)}. \tag{3.17}$$

In this expression for the wave, the first term is the incident wave and the second term is the reflected wave with $r$ as the reflection coefficient. If we apply our absorbing boundary condition (3.9) to this wave, we obtain

$$B\Psi = \left[-k + \frac{ma}{\hbar}\right] e^{-i(\omega t - kx)} + r\left[k + \frac{ma}{\hbar}\right] e^{-i(\omega t + kx)} = 0. \tag{3.18}$$

Therefore, the reflection coefficient is

$$R = |r| = \left| \frac{-k + \frac{ma}{\hbar}}{k + \frac{ma}{\hbar}} \right|. \tag{3.19}$$

Note that $|r|$ is always less than one if $\hbar k$ and $a_i$ have the same sign. The general form of the reflection for the full absorbing boundary condition (3.10) is

$$R = \prod_{l=1}^{p} \left| \frac{-k + \frac{ma_l}{\hbar}}{k + \frac{ma_l}{\hbar}} \right|. \tag{3.20}$$

This expression for the reflection shows that where $ma_l/\hbar = k$, the absorbing boundary condition (3.10) is perfectly absorbing since $R = 0$. Otherwise, $|r| < 1$ and all the incident components of the wave are reduced in amplitude in the reflected wave, implying absorption of the incident wave. To minimize the reflection produced by the absorbing boundary condition, we can do two things. Since $|r|$ is less than one, the larger the value of $p$ in (3.20), the smaller the value of the reflection. Hence, we seek a higher order absorbing boundary condition, where feasible, to minimize the reflection. Also, where the incident wave is composed of several wave packets with different group velocities, choosing $a_l$ to coincide with the incident group velocities will decrease the value of the reflection given by (3.20).

**3.6. Well-posedness of the new absorbing boundary condition.** Of course, it is also very important to show that these boundary conditions given by (3.10) generate well-posed initial boundary value problems when coupled with the Schrödinger equation. A well-posed problem is one that does not admit either solutions with exponentially growing amplitudes anywhere in the domain or spurious solutions generated from the boundary. Much is known about the well-posedness of the Schrödinger equation; see, e.g., [18]. In this section, our discussion of well-posedness will be based on the theory developed by Kreiss [17] for wave equations.

The Kreiss condition [17] for wave equations states that for well-posedness, the problem must not admit any eigenvalues or any generalized eigenvalues. Eigenvalues are those complex values $s$ that simultaneously satisfy both the dispersion relation of the interior differential equation and the symbol of the boundary condition, such that $\mathrm{Re}(s) > 0$. If such eigenvalues exist, then the initial boundary value problem admits a normal mode $\mathrm{e}^{st}$, which grows unboundedly, and is hence unstable. Generalized eigenvalues are complex values $s$ that also satisfy the dispersion relation and the symbol of the boundary condition, but where $\mathrm{Re}(s) = 0$ *and* the group velocity of the normal mode is $\geq 0$ ($\leq 0$) on the left-hand (right-hand) boundary. If there are any generalized eigenvalues, then the boundary condition will admit a spurious traveling wave solution which will propagate energy into the interior domain.

Following the example worked out by Engquist and Majda [2] for both constant coefficient and slowly varying coefficient wave equations, we use the general algebraic normal mode analysis for checking well-posedness, specialized for the Schrödinger equation, as follows.

PROPOSITION 3.1. *The initial boundary value problem for the Schrödinger equation is well-posed if there are no solutions to the frozen coefficient half-space problems of the form*

$$\tilde{\Psi}(s) = e^{st+kx} \tag{3.21}$$

*with* Re $s \geq 0$ (*where* $s$ *is complex*). *Here the half-space we are considering is* $x \geq 0$ *with the boundary at* $x = 0$ *and taking the positive branch of the square root function. A solution where* Re $s > 0$ *would be an eigenvalue. A solution where* Re $s = 0$ *would be a generalized eigenvalue. Note that the dispersion relation for the interior solutions has been substituted for the wave number in* (3.21). *The solutions would have to satisfy*

$$i\hbar \frac{\partial \tilde{\Psi}}{\partial t}(s) = -\frac{\hbar^2}{2m} \frac{\partial^2 \tilde{\Psi}(s)}{\partial x^2} + V\tilde{\Psi}(s) \tag{3.22}$$

*and*

$$\prod_{l=1}^{p} \left( i\frac{\partial}{\partial x} - \frac{ma_l}{\hbar} \right) \tilde{\Psi}(s) = 0. \tag{3.23}$$

Specifically, the above criterion corresponds to waves impinging on the left-hand boundary, but the result holds equally for the right-hand boundary. For $p = 1$, if a function of the form (3.21) satisfies (3.22), then $i\hbar s = -\frac{\hbar^2}{2m}k^2 + V$. Applying the boundary condition (3.23) with $p = 1$, we get $ik - \frac{ma_1}{\hbar} = 0$. Combining the two equations leads to

$$s = \frac{i}{\hbar} \left( \frac{m{a_1}^2}{2} + V \right). \tag{3.24}$$

From (3.24), it is obvious that

$$\text{Re } s = 0, \tag{3.25}$$

since $s$ is wholly imaginary. This implies that there are no eigenvalues. Also, since the boundary condition is constructed such that the group velocity is $\leq 0$ on the left-hand boundary, there are also no generalized eigenvalues which will propagate waves into the interior. However, there is a generalized eigenvalue with zero group velocity which remains on the boundary. Therefore, if there are any instabilities which might be admitted by the generalized eigenvalue of the absorbing boundary condition, they would not propagate into the interior of the solution, and thus they will not affect the interior solution. Therefore, the boundary condition is well-posed with the exception of the zero group velocity generalized eigenvalue for $p = 1$. To see that the boundary condition is also well-posed for $p > 1$, consider the product form of the boundary condition (3.23). An eigenvalue or a generalized eigenvalue must be a solution of (3.23). Therefore, at least one factor in (3.23) must be zero. That is, (3.24) is satisfied for some $a_1$. Then the same discussion as above shows that $s = 0$ is the only generalized eigenvalue for $p > 1$.

**3.7. Higher dimensions.** It is straightforward to extend the general absorbing boundary condition (3.10) to two or three dimensions. Consider the Schrödinger equation in two dimensions,

$$i\hbar \frac{\partial \Psi(x,y,t)}{\partial t} = -\frac{\hbar^2}{2m} \left( \frac{\partial^2 \Psi(x,y,t)}{\partial x^2} + \frac{\partial^2 \Psi(x,y,t)}{\partial y^2} \right) + V(x,y)\Psi(x,y,t), \tag{3.26}$$

where $m, V(x,y)$, and $\Psi(x,y,t)$ are defined as before. The interior numerical solution for the two-dimensional Schrödinger equation is given by Galbraith, Ching, and Abraham [5]. Kuska developed a two-dimensional version of his boundary condition as a straightforward extension of his one-dimensional version (3.5) [19].

Following essentially the same procedure as that used to derive (3.10), consider a two-dimensional plane wave of the form

$$\Psi(x,t) = \mathrm{e}^{-i(\omega t - k_x x - k_y y)}, \tag{3.27}$$

where $\omega$ is the frequency of the wave and $k_x$ and $k_y$ are the wave vectors in the $x$ and $y$ directions, respectively. Equivalently, $k_x = k\cos\phi$ and $k_y = k\sin\phi$ where $\phi$ is the angle of the direction of $k$ measured from the normal (pointing away from the interior) of the $x = a$ boundary. ($a$ can be 0 or $L$.) Then we have the dispersion relation

$$\hbar^2 k_x^2 + \hbar^2 k_y^2 = 2m\left[\omega\hbar - V\right], \tag{3.28}$$

assuming that the potential $V$ is a constant in the neighborhood of the boundaries. This gives us the following group velocities:

$$(C_x, C_y) = \left(\frac{\partial\omega}{\partial k_x}, \frac{\partial\omega}{\partial k_y}\right) = \left(\frac{\hbar k_x}{m}, \frac{\hbar k_y}{m}\right). \tag{3.29}$$

Therefore, on the $x = L$ boundary, the two-dimensional version of (3.8) is, using the same argument as in section 3.3,

$$\frac{\hbar k_x}{m} \equiv a_x, \tag{3.30}$$

where $a_x$ is the $x$ component of a two-dimensional group velocity such that $a_x = a\cos\theta$. The angle is the direction of group velocity measured from the normal of the $x = L$ boundary, as $\phi$ above. Since the corresponding differential operator to $k_x$ is $-i\partial/\partial x$, our general absorbing boundary condition in two dimensions becomes

$$\prod_{l=1}^{p}\left(i\frac{\partial}{\partial x} + \frac{m a_l \cos\theta_l}{\hbar}\right)\Psi = 0. \tag{3.31}$$

Actually, $\cos\theta_l$ can be absorbed by $a_l$ leaving $a_l$ as the only necessary parameter. Again, for waves traveling to the left and impinging on the $x = 0$ boundary, $a_l$ would simply be substituted by $-a_l$ in (3.31).

As before, we can derive the reflection coefficient produced by the two-dimensional absorbing boundary condition. If we consider an incident wave of the form

$$\Psi = \mathrm{e}^{-i(\omega t - k\cos\phi x - k\sin\phi y)} + r\mathrm{e}^{-i(\omega t + k\cos\phi x - k\sin\phi y)}, \tag{3.32}$$

where $r$ is the amplitude of the reflected component, then absorbing boundary condition (3.31) would generate the following reflection coefficient:

$$R = \prod_{l=1}^{p}\left|\frac{-k\cos\phi + \frac{m a_l\cos\theta_l}{\hbar}}{k\cos\phi + \frac{m a_l\cos\theta_l}{\hbar}}\right|. \tag{3.33}$$

We would choose $\cos\theta_l$ and $a_l$ to minimize the reflection coefficient.

Let us consider a practical implementation of this two-dimensional absorbing boundary condition with $p = 3$. Then, in wave vector format, (3.31) takes the following form:

$$\left(-k_x + \frac{ma_{x1}}{\hbar}\right)\left(-k_x + \frac{ma_{x2}}{\hbar}\right)\left(-k_x + \frac{ma_{x3}}{\hbar}\right) = 0. \tag{3.34}$$

This simplifies to the relation, with the substitution of terms of $k_x^2$ with (3.28),

$$\hbar k_x = \frac{2m\tilde{h}_1(\hbar\omega - V) - \hbar^2\tilde{h}_1 k_y^2 + \tilde{h}_3}{2m(\hbar\omega - V) - \hbar^2 k_y^2 + \tilde{h}_2}, \tag{3.35}$$

where

$$\begin{aligned}
\tilde{h}_1 &= m\left(a_{x1} + a_{x2} + a_{x3}\right), \\
\tilde{h}_2 &= m^2 a_{x1}a_{x2}a_{x3}\left(\frac{1}{a_{x1}} + \frac{1}{a_{x2}} + \frac{1}{a_{x3}}\right), \\
\tilde{h}_3 &= m^3 a_{x1}a_{x2}a_{x3}.
\end{aligned}$$

In explicit differential form, where we have substituted for the duals in the symbol (3.35) with their respective differential operators, this absorbing boundary condition evaluated at the $x = L$ boundary would have the form

$$\begin{aligned}
\Bigg[-\hbar^3 i\frac{\partial^3\Psi}{\partial x\partial y^2} + 2m\hbar^2\frac{\partial^2\Psi}{\partial t\partial x} - \hbar^2\tilde{h}_1\frac{\partial^2\Psi}{\partial y^2} - 2m\hbar\tilde{h}_1 i\frac{\partial\Psi}{\partial t} \\
+\hbar i(2mV - \tilde{h}_2)\frac{\partial\Psi}{\partial x} + (2m\tilde{h}_1 V - \tilde{h}_3)\Psi\Bigg]\Bigg|_{x=L} = 0.
\end{aligned} \tag{3.36}$$

If $a_{xj} = \hbar k_{0x}/m$, then we recover the absorbing boundary condition given by Kuska [19, equation (11)], with $k_{0x}$ being defined as the $x$ component of the initial wave vector $k_0$ [19].

**4. Numerical tests of absorbing boundary conditions.** In this section, we will use a finite-difference scheme to test the effectiveness of various orders of the general absorbing boundary condition (3.10). This scheme will be used with several initial distributions of (i) a single Gaussian distribution modulating a traveling plane wave, (ii) the sum of two Gaussian distributions modulating two waves traveling at different initial group velocities, and (iii) a narrow Gaussian pulse approximated by a Gaussian distribution with small initial spread modulating a single plane wave. The amount of reflection generated by the absorbing boundary conditions will be compared at the different orders to determine their relative effectiveness.

**4.1. Schrödinger equation implicit interior scheme.** For the numerical results, an implicit finite-difference interior scheme will be used to numerically solve the Schrödinger equation. The spatial domain of the numerical solution of (3.1) is $x = x_j = j\epsilon$, with $j \in [0, \mathcal{J}]$, where $\epsilon$ is the spatial mesh width. Therefore, the left-most boundary is $x = 0$ and the right-most boundary is $x = \mathcal{J}\epsilon = L$. Similarly, the time variable has the range $t = t_n = n\delta$, with $n = 0, 1, 2, \ldots, N$. $\Psi(x_j, T = N\delta)$ are the last calculated wave-function values. We will discuss later how to choose $N$. Along the same lines, the discretization of the wave function is $\Psi_j^n = \Psi(x_j, t_n)$.

We will use the following implicit scheme [6]:

$$\begin{aligned}&\Psi_{j+1}^{n+1}+\left(-2+\frac{4im}{\hbar\lambda}-\frac{2m\epsilon^2V_j}{\hbar^2}\right)\Psi_j^{n+1}+\Psi_{j-1}^{n+1}\\&=-\Psi_{j+1}^{n}+\left(2+\frac{4im}{\hbar\lambda}+\frac{2m\epsilon^2V_j}{\hbar^2}\right)\Psi_j^{n}-\Psi_{j-1}^{n},\end{aligned}\tag{4.1}$$

where $\lambda=\delta/\epsilon^2$. The discretization $V_j$ implies the value $V(x_j)$. The implicit scheme is based on the calculation of the next time step of the integration using only the previous time step. This scheme preserves the unitarity of the wave-function and meets the von Neumann test requirement [8].

**4.2. Numerical schemes for the absorbing boundary condition.** To numerically implement the absorbing boundary conditions, we need to discretize the differential operators to produce finite-difference schemes. We will consider a number of orders ($p$) of the general absorbing boundary condition (3.10).

**4.2.1. The $p=2$ absorbing boundary condition.** This boundary condition is based on (3.12). This boundary condition is equivalent to the absorbing boundary condition (3.4) presented by Shibata [23]. Translated into explicit differential form, the absorbing boundary condition becomes

$$\pm i\hbar\Psi_x-i\hbar c_1\Psi_t+(c_1V-c_2)\Psi=0,\tag{4.2}$$

where

$$c_1=\frac{2}{a_1+a_2},\qquad c_2=\frac{ma_1a_2}{a_1+a_2}.\tag{4.3}$$

The positive sign on the first term refers to the boundary condition applied to the $x=0$ boundary and the negative sign refers to the $x=L$ boundary.

The following finite-difference discretizations [19] will be used for the differential operators in (4.2):

$$\Psi\approx\frac{(Z+I)}{2}\frac{(J^{\pm}+I)}{2}\Psi_j^n,\tag{4.4}$$

$$\Psi_x\approx\pm\frac{(Z+I)}{2}\frac{(J^{\pm}-I)}{\epsilon}\Psi_j^n,\tag{4.5}$$

$$\Psi_t\approx\frac{(J^{\pm}+I)}{2}\frac{(Z-I)}{\delta}\Psi_j^n,\tag{4.6}$$

where the top sign of a double-signed term refers to the $x=0$ boundary condition and the bottom sign refers to the $x=L$ boundary condition (from the negative and positive values for wave vector $k$, denoting left- and right-traveling waves, respectively). This abbreviation convention will be used throughout. In the above, the shift operators $J\Psi_j^n=\Psi_{j+1}^n$, $I\Psi_j^n=\Psi_j^n$, $J^-\Psi_j^n=\Psi_{j-1}^n$ were used. Similar shift operators were also used for time operations—$Z\Psi_j^n=\Psi_j^{n+1}$, $Z^-\Psi_j^n=\Psi_j^{n-1}$.

Using these discretizations in (4.2) yields the following $p=2$ absorbing boundary condition:

$$\left(\frac{i\hbar}{2\epsilon}-\frac{i\hbar c_1}{2\delta}+\frac{(c_1V_{(0,\mathcal{J})}-c_2)}{4}\right)\Psi_{(1,\mathcal{J}-1)}^{n+1}$$

$$
\begin{aligned}
&+\left(-\frac{i\hbar}{2\epsilon}-\frac{i\hbar c_1}{2\delta}+\frac{(c_1V_{(0,\mathcal{J})}-c_2)}{4}\right)\Psi^{n+1}_{(0,\mathcal{J})}\\
&=\left(-\frac{i\hbar}{2\epsilon}-\frac{i\hbar c_1}{2\delta}-\frac{(c_1V_{(0,\mathcal{J})}-c_2)}{4}\right)\Psi^{n}_{(1,\mathcal{J}-1)}\\
&+\left(\frac{i\hbar}{2\epsilon}-\frac{i\hbar c_1}{2\delta}-\frac{(c_1V_{(0,\mathcal{J})}-c_2)}{4}\right)\Psi^{n}_{(0,\mathcal{J})}. \qquad (4.7)
\end{aligned}
$$

The abbreviation for the wave function, $\Psi^{n+1}_{(1,\mathcal{J}-1)}$, denotes that the discrete scheme uses the value $\Psi^{n+1}_1$ on the $x=0$ boundary and $\Psi^{n+1}_{\mathcal{J}-1}$ on the $x=L$ boundary.

**4.2.2. The $p=3$ absorbing boundary condition.** This boundary condition is based on (3.14). A special case of this boundary condition would yield the absorbing boundary condition (3.15) considered by Kuska [19]. Rewritten in explicit differential form, (3.14) has the form

$$
\pm i\hbar\left(\frac{h_2}{2m}-V\right)\Psi_x\mp\hbar^2\Psi_{tx}-i\hbar h_1\Psi_t-\left(\frac{h_3}{2m}-h_1V\right)\Psi=0, \qquad (4.8)
$$

where $h_i$ are defined in the previous section.

The finite-difference discretizations given in (4.4) to (4.6), along with the following discretization [19], will be used for the differential operators in (4.8):

$$
\Psi_{tx}\approx\pm\frac{(Z-I)}{\delta}\frac{(J^{\pm}-I)}{\epsilon}\Psi^n_j. \qquad (4.9)
$$

These discretizations applied to (4.8) yield the following $p=3$ absorbing boundary condition:

$$
\begin{aligned}
&\left(\frac{a}{2\epsilon}-\frac{b}{\delta\epsilon}-\frac{c}{2\delta}-\frac{d}{4}\right)\Psi^{n+1}_{(1,\mathcal{J}-1)}+\left(-\frac{a}{2\epsilon}+\frac{b}{\delta\epsilon}-\frac{c}{2\delta}-\frac{d}{4}\right)\Psi^{n+1}_{(0,\mathcal{J})}\\
&=\left(-\frac{a}{2\epsilon}-\frac{b}{\delta\epsilon}-\frac{c}{2\delta}+\frac{d}{4}\right)\Psi^{n}_{(1,\mathcal{J}-1)}+\left(\frac{a}{2\epsilon}+\frac{b}{\delta\epsilon}-\frac{c}{2\delta}+\frac{d}{4}\right)\Psi^{n}_{(0,\mathcal{J})}, \qquad (4.10)
\end{aligned}
$$

where $a=i\hbar\left(\frac{h_2}{2m}-V_{(0,\mathcal{J})}\right)$, $b=\hbar^2$, $c=i\hbar h_1$, $d=\left(\frac{h_3}{2m}-h_1V_{(0,\mathcal{J})}\right)$.

**4.2.3. The $p=4$ absorbing boundary condition.** Equation (3.15) for $p=4$ leads to the differential absorbing boundary condition

$$
p_1\Psi_{tt}\pm p_2\Psi_{tx}+p_3\Psi_t\pm p_4\Psi_x+p_5\Psi=0, \qquad (4.11)
$$

where $p_1=-4m^2\hbar^2$, $p_2=2mg_1\hbar^2$, $p_3=2mi\hbar g_2-8m^2i\hbar V_{(0,\mathcal{J})}$, $p_4=2mi\hbar g_1V_{(0,\mathcal{J})}-i\hbar g_3$, $p_5=4m^2(V_{(0,\mathcal{J})})^2-2mg_2V_{(0,\mathcal{J})}+g_4$, where $g_i$ are defined as in section 3. To discretize this differential boundary condition, we will use

$$
\Psi_{tt}\approx-\frac{(Z^{-}-I)}{\delta}\frac{(Z-I)}{\delta}\Psi^n_j \qquad (4.12)
$$

along with the discretizations given in (4.4) to (4.6) and (4.9). The result of these discretizations in (4.11) yields the following $p=4$ absorbing boundary condition:

$$
\begin{aligned}
&\left(\frac{p_2}{\delta\epsilon}+\frac{p_3}{2\delta}+\frac{p_4}{2\epsilon}+\frac{p_5}{4}\right)\Psi^{n+1}_{(1,\mathcal{J}-1)}+\left(\frac{p_1}{\delta^2}-\frac{p_2}{\delta\epsilon}+\frac{p_3}{2\delta}-\frac{p_4}{2\epsilon}+\frac{p_5}{4}\right)\Psi^{n+1}_{(0,\mathcal{J})}\\
&=\left(\frac{p_2}{\delta\epsilon}+\frac{p_3}{2\delta}-\frac{p_4}{2\epsilon}-\frac{p_5}{4}\right)\Psi^{n}_{(1,\mathcal{J}-1)}+\left(2\frac{p_1}{\delta^2}-\frac{p_2}{\delta\epsilon}+\frac{p_3}{2\delta}+\frac{p_4}{2\epsilon}-\frac{p_5}{4}\right)\Psi^{n}_{(0,\mathcal{J})}\\
&+\left(-\frac{p_1}{\delta^2}\right)\Psi^{n-1}_{(0,\mathcal{J})}. \qquad (4.13)
\end{aligned}
$$

Note that two previous time levels are needed to calculate the subsequent time level in (4.13)

**4.3. Numerical results.** The initial conditions used for all numerical calculations is a Gaussian distribution (either singularly or in combinations):

$$\Psi_j^0 = \mathrm{e}^{-(x_j-\xi)^2/2{\sigma_0}^2}\mathrm{e}^{iK_0x_j}. \tag{4.14}$$

In all the following calculation results, unless otherwise stated, $m = 0.5$ and $\hbar = 1$. Also, the potential $V$ will be set to zero for all calculations.

What does this choice for initial conditions tell us about the applicability of the boundary conditions with respect to completely general initial conditions? We note that any general initial conditions can be expressed in terms of a Fourier series, and a single Fourier mode is essentially a plane wave. Therefore, since the Gaussian distribution's carrier wave is a plane wave, if the boundary conditions are well behaved for various frequencies of plane waves in our examples, then the boundary condition would be expected to be well behaved for any arbitrary choice of initial conditions whose Fourier modes are dominant at the same frequencies.

**4.3.1. Tests of the reflection properties of the general absorbing boundary condition.** We will compare the relative properties, in terms of reflection, of different orders of the general absorbing boundary condition (3.10), with respect to each other and with respect to the exact solution. Also, the effectiveness of the more general form of (3.10) will be considered in comparison with the published absorbing boundary conditions of Shibata [23] and Kuska [19].

The reflection ratio $r$ at $t_n$ was calculated as [19]

$$r = \frac{\sum_{j=0}^{\mathcal{J}} |\Psi_j^n|^2}{\sum_{j=0}^{\mathcal{J}} |\Psi_j^0|^2}. \tag{4.15}$$

This $r$ is similar to the reflection coefficient $|r|$ in (3.19). Here, $r$ is the ratio of the integration of the squared amplitude of the reflected wave-function over the initial wave-function (essentially, the ratio of the reflected wave with respect to the initial wave). Since our wave-functions are discrete, the integration is a summation over the domain. When the wave is completely reflected, then $r = 1$, whereas if the wave is completely absorbed, then $r = 0$, after the initial wave has passed through the absorbing boundary condition. To compare the different schemes, we will plot the reflection ratio as a function of time. This method of comparison is most useful when only one wave is passing through a boundary at a time. When no waves are passing through either boundary and any traveling waves are presently only in the interior of the domain, then the reflection ratio as a function of time is a plateau whose value measures the total wave amplitude remaining in the interior of the domain. Waves smoothly passing through a boundary are represented by a smoothly decreasing reflection ratio as a function of time. As the waves present in the interior domain are diminished by passing through the absorbing boundary conditions, $r$ eventually goes to zero. The reflection ratio values that we are primarily interested in are the midpoints of the first plateau, when the Gaussian distribution has passed through the $x = L$ boundary and any waves reflected are still in the interior of the domain and have not yet reached the $x = 0$ boundary. Obviously, for more arbitrary wave solutions, this method of comparison would not be adequate on small domains, since we would not be able to tell when the particular waves we are interested in are passing through the boundaries.

**4.3.2. Single Gaussian distribution.** The first set of comparisons will use an initial distribution of a single Gaussian distribution as given by (4.14). Figures 4.1 to 4.6 show plots of reflection ratio as a function of time for $K_0 = 5,\ 15,$ and 30, with $L = 10, \sigma_0 = L/10$, and $\xi = 3L/4$ (with an exception for $K_0 = 5$ where the range of $x$ used was $[-20, 10]$ so that any reflection from the $x = 0$ boundary does not affect the results). For all computations, $\delta = 0.0001$ and $a_i = \hbar K_0/m$ for the absorbing boundary conditions. The various orders of the general absorbing boundary condition and different spatial sizes of the grid are compared. Listed on the plots are the value of $p$ of the boundary condition and the value of $\mathcal{J}$ from which $\epsilon = L/\mathcal{J}$ is determinable. The "im" implies that the scheme used is an implicit scheme. The relative values of reflection ratios for the different schemes are shown in Table 4.1 at various time slices, chosen to coincide with the midpoints of the reflection ratio plateaus in Figures 4.1 to 4.6.

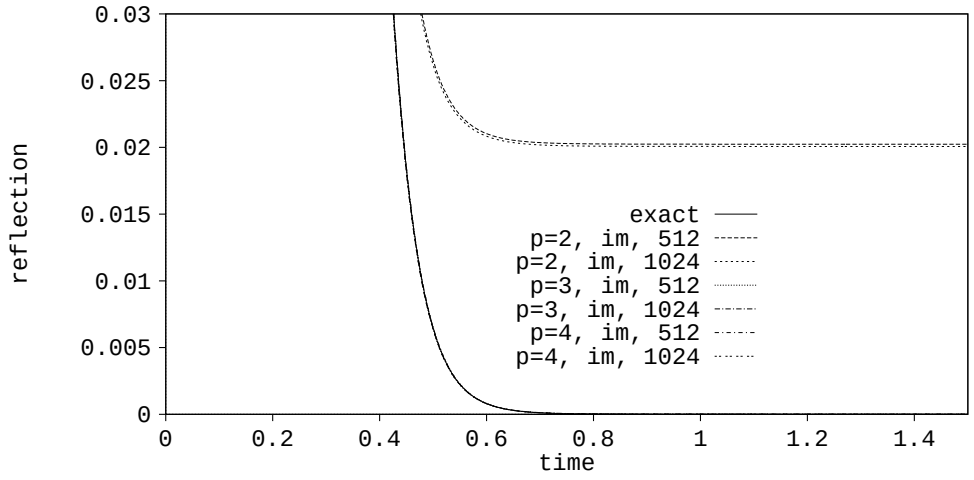


FIG. 4.1. *Reflection ratio as a function of time for* $K_0 = 5.0$. *See Figure* 4.2 *for a close-up of the* $p = 2$ *and* $p = 3$ *plots.*

It is obvious from the values in Table 4.1 and from the plots in Figures 4.1 to 4.6 that the reflection ratio is lower for the higher order absorbing boundary conditions. It is a bit unexpected that the $p = 3$ absorbing boundary condition performed better than the $p = 4$, which we would expect to have a lower reflection ratio value as predicted by (3.20). This will be discussed later. Also, the smaller the grid spacing $\epsilon$, the less reflection produced by the absorbing boundary condition.

Now, assume that we use the same Gaussian distribution calculation, again using the implicit interior schemes, but vary the interpolated group velocities of the absorbing boundary condition for $p = 3$ and $p = 4$ as follows: $a_i = (1 + \zeta)\frac{\hbar K_0}{m}$, where $\zeta$ is the variation of group velocity. The rationale for this type of calculation is twofold. First, as the Gaussian distribution evolves via the Schrödinger equation, the distribution in momentum space spreads [6]. Also, a calculation of the group velocity at the $x = L$ boundary as the single Gaussian distribution passes through the boundary will reveal that the real component of the group velocity of the distribution increases and then decreases after the peak of the distribution has passed through the boundary, as we can see in Figure 4.7, whereas the imaginary component simply decreases, as in

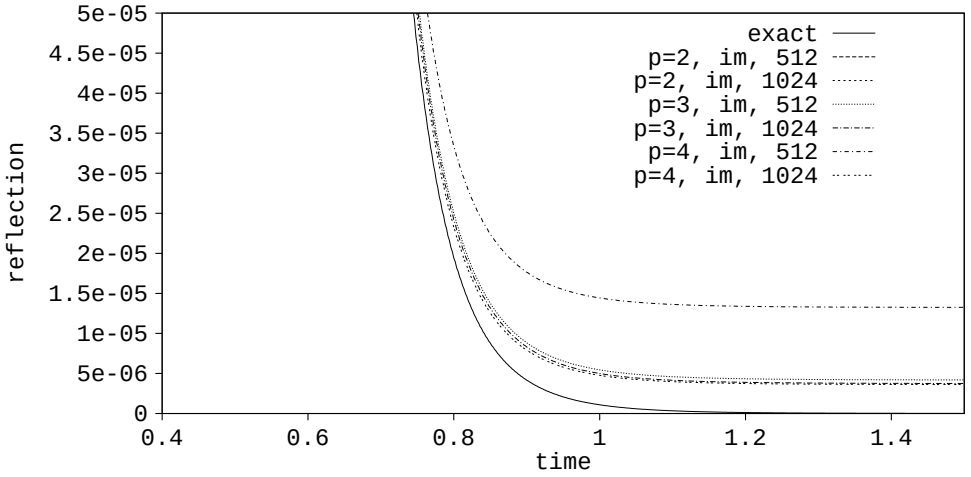


FIG. 4.2. *Close-up of the reflection ratio as a function of time for* $K_0 = 5.0$.

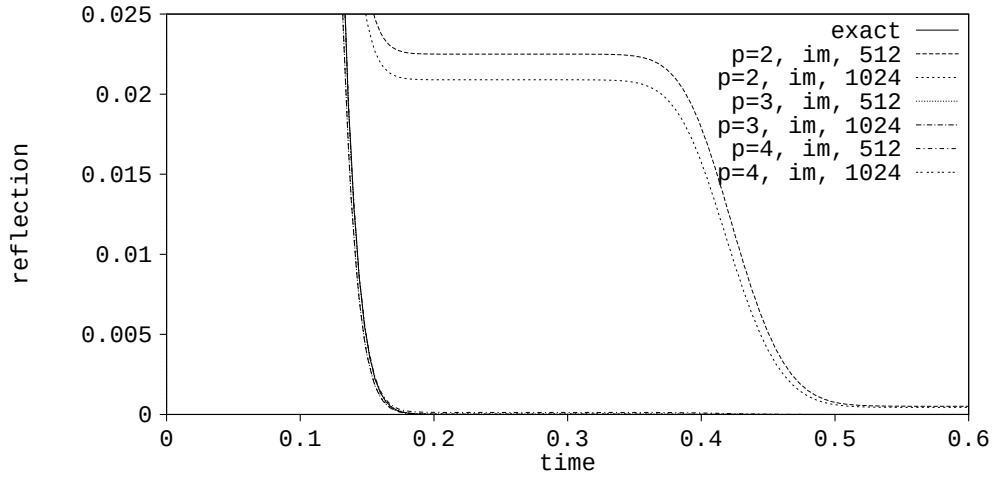


FIG. 4.3. *Reflection ratio as a function of time for* $K_0 = 15.0$. *See Figure* 4.4 *for a close-up of the* $p = 2$ *and* $p = 3$ *plots.*

Figure 4.8. Hence, we would not expect the initial value of the group velocity to give the best results for the absorbing boundary condition. Also, each order of the general absorbing boundary condition will interpolate the exact dispersion relation for the Schrödinger equation differently. Hence the properties of each order of the absorbing boundary condition will be different according to how the initial distribution evolves with respect to the form of the interpolation.

However, since the higher order absorbing boundary conditions have multiple degrees of freedom, we will use a simple one degree of freedom test of the properties of the $p = 3$ and $p = 4$ absorbing boundary conditions. Using $\zeta$ as the variable and the values of $a_i$ shown above, we obtain the results shown in Figure 4.9. Obviously, the higher values of $a_i$ allow the $p = 3$ absorbing boundary condition to reduce reflection ratio, reaching its optimal performance at $a_i \approx 1.39\hbar K_0/m$. For even higher values of $a_i$, the $p = 4$ absorbing boundary condition improves its absorption properties to the

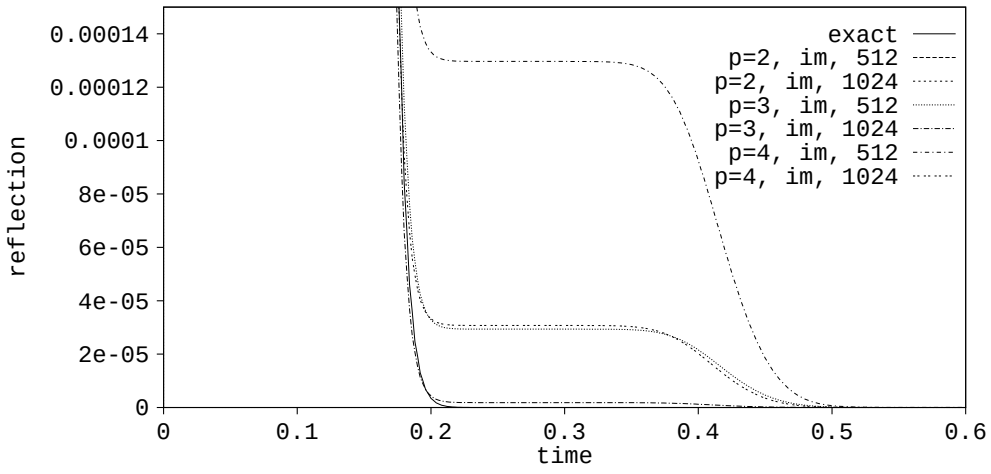


FIG. 4.4. *Close-up of the reflection ratio as a function of time for* $K_0 = 15.0$.

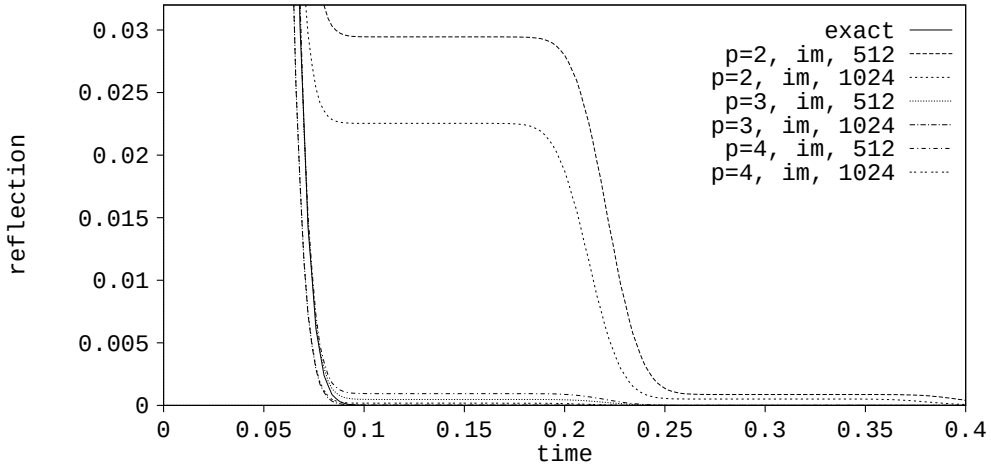


FIG. 4.5. *Reflection ratio as a function of time for* $K_0 = 30.0$. *See Figure* 4.6 *for a close-up of the* $p = 2$ *and* $p = 3$ *plots.*

point were its reflection ratio is only a few times higher than the optimal value for the $p = 3$ absorbing boundary condition.

**4.3.3. Double Gaussian distribution.** The next series of comparisons will use an initial distribution composed of two Gaussian distributions with different initial group velocities. Initially, the distribution has the form

$$\Psi_j^0 = \frac{e^{-(x_j-\xi)^2/2\sigma_0{}^2} e^{iK_0 x_j} + e^{-(x_j-\xi)^2/2\sigma_0{}^2} e^{iK_1 x_j}}{\sqrt{2}}. \tag{4.16}$$

For our calculations, $K_0 = 25, K_1 = 5, \epsilon = 10/512$, $\delta = 0.0001, \sigma_0 = 1$, and $\xi = 7.5$. The calculation was carried out using the implicit solution for the interior of the domain and the $p = 3$ and $p = 4$ absorbing boundary conditions. The key of the plots contains the value of $p$ and a series of ones and zeros for the values of $a_1, a_2, a_3$

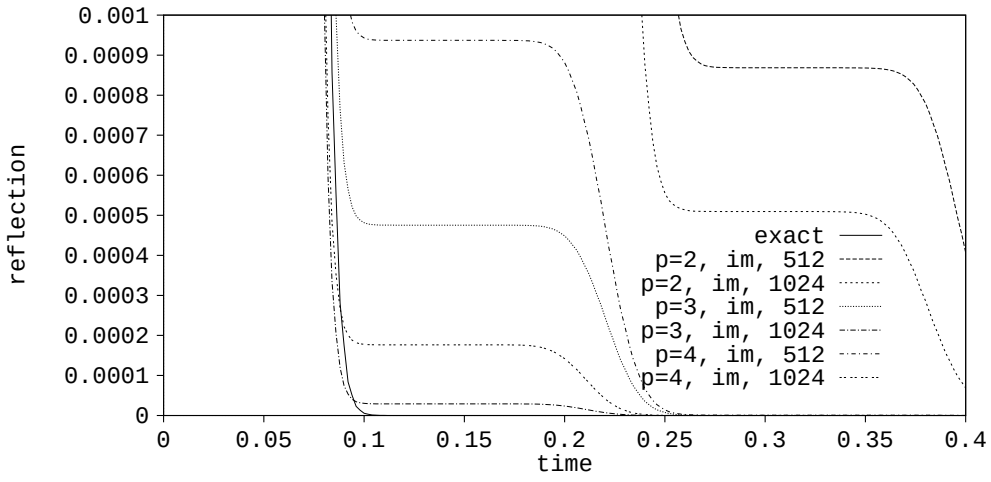


FIG. 4.6. *Close-up of the reflection ratio as a function of time for* $K_0 = 30.0$.

TABLE 4.1
*Comparison of reflection ratios vs. different schemes for single Gaussian.*

| *No.* | *Implicit Scheme* | $K_0$ | *time* | $r$ |
|---|---|---|---|---|
| 1 | $p = 2, \mathcal{J} = 512$ | 5.0 | 1.5 | $2.024 \times 10^{-2}$ |
| 2 | $p = 2, \mathcal{J} = 1024$ | 5.0 | 1.5 | $2.007 \times 10^{-2}$ |
| 3 | $p = 3, \mathcal{J} = 512$ | 5.0 | 1.5 | $4.193 \times 10^{-6}$ |
| 4 | $p = 3, \mathcal{J} = 1024$ | 5.0 | 1.5 | $3.750 \times 10^{-6}$ |
| 5 | $p = 4, \mathcal{J} = 512$ | 5.0 | 1.5 | $1.325 \times 10^{-5}$ |
| 6 | $p = 4, \mathcal{J} = 1024$ | 5.0 | 1.5 | $3.618 \times 10^{-6}$ |
| 7 | $p = 2, \mathcal{J} = 512$ | 15.0 | 0.3 | $2.250 \times 10^{-2}$ |
| 8 | $p = 2, \mathcal{J} = 1024$ | 15.0 | 0.3 | $2.090 \times 10^{-2}$ |
| 9 | $p = 3, \mathcal{J} = 512$ | 15.0 | 0.3 | $2.935 \times 10^{-5}$ |
| 10 | $p = 3, \mathcal{J} = 1024$ | 15.0 | 0.3 | $1.829 \times 10^{-6}$ |
| 11 | $p = 4, \mathcal{J} = 512$ | 15.0 | 0.3 | $1.297 \times 10^{-4}$ |
| 12 | $p = 4, \mathcal{J} = 1024$ | 15.0 | 0.3 | $3.073 \times 10^{-5}$ |
| 13 | $p = 2, \mathcal{J} = 512$ | 30.0 | 0.15 | $2.945 \times 10^{-2}$ |
| 14 | $p = 2, \mathcal{J} = 1024$ | 30.0 | 0.15 | $2.254 \times 10^{-2}$ |
| 15 | $p = 3, \mathcal{J} = 512$ | 30.0 | 0.15 | $4.754 \times 10^{-4}$ |
| 16 | $p = 3, \mathcal{J} = 1024$ | 30.0 | 0.15 | $2.907 \times 10^{-5}$ |
| 17 | $p = 4, \mathcal{J} = 512$ | 30.0 | 0.15 | $9.370 \times 10^{-4}$ |
| 18 | $p = 4, \mathcal{J} = 1024$ | 30.0 | 0.15 | $1.765 \times 10^{-4}$ |

(and $a_4$ if the scheme is $p = 4$), respectively. A one indicates that the corresponding value of $a_j$ equals $\frac{\hbar K_1}{m}$ and a zero indicates that $a_j = \frac{\hbar K_0}{m}$. Therefore, $0, 1, 1$ implies that $a_1 = \frac{\hbar K_0}{m}$ and $a_2 = a_3 = \frac{\hbar K_1}{m}$ for that scheme. The fluctuating amplitudes in the plots are due to the interference patterns formed by the two waves traveling at two different group velocities. When the waves no longer overlap, such as at $t = 0.2$, the fluctuations are absent (except for any interaction between the slower wave and reflections off the absorbing boundary condition).

For the double Gaussian calculations, the range of $x$ over which the reflection ratio, $r$, was calculated was $-90 \leq x \leq 10]$, with the boundaries placed at $x = -90$ and $x = 10$. This placement was necessary to prevent any possible multiple reflections produced by the faster moving distribution from affecting the slower distribution.

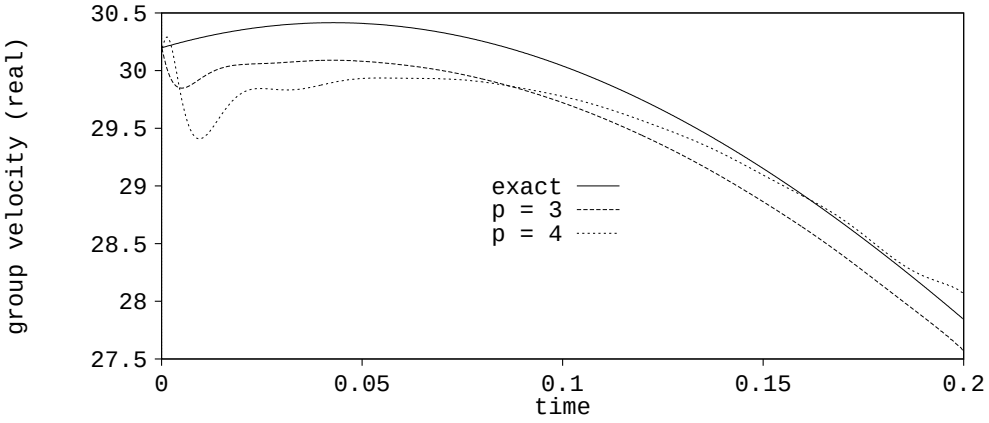


FIG. 4.7. *Measured group velocity as a function of time at the $x = L$ boundary for $K_0 = 15.0$ (real component).*

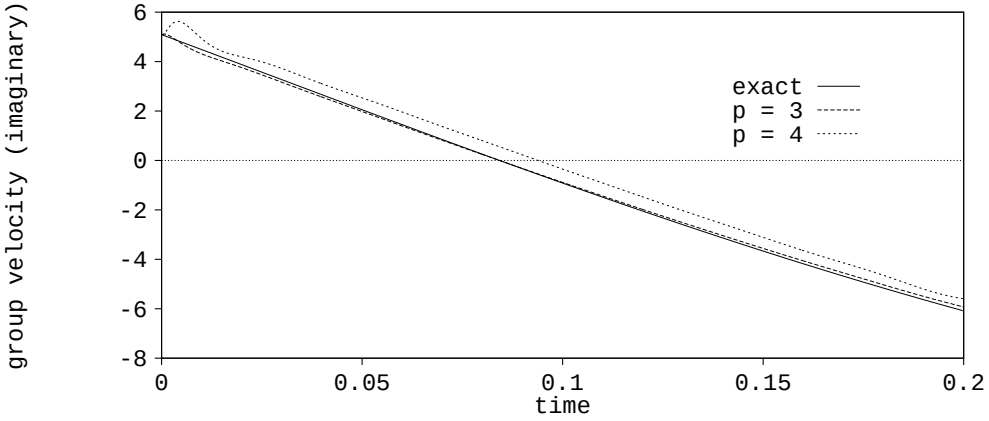


FIG. 4.8. *Measured group velocity as a function of time at the $x = L$ boundary for $K_0 = 15.0$ (imaginary component).*

Also, the two respective reflection waves may be distinguished. The values of the reflection ratio as a function of time are given in Figure 4.10. Also, for comparison, the values of the reflection ratio at $n = 8400$ ($t = 0.84$) are given in Table 4.2. At $t = 0.84$, both the initial Gaussian distribution components have passed through the $x = 10$ boundary and only the reflected components are present in the interior domain and have not yet reached the other boundary. Obviously, when the $a_i$'s are tuned to both the initial group velocities, $\hbar K_0/m$ and $\hbar K_1/m$, rather than to just one of these values, the amount of reflection generated by the absorbing boundary conditions drops by up to two orders of magnitude, with the least amount of reflection being produced by scheme 4 in Table 4.2.

We know from the distribution in momentum space that the initial Gaussians have a distribution in momentum space peaked about $\hbar K_0$ and about $\hbar K_1$. Therefore, for optimal absorbing boundary conditions, the $a_j$'s that we use should also be distributed around the $\hbar K_0/m$, as well as about $\hbar K_1/m$, to absorb the components that are

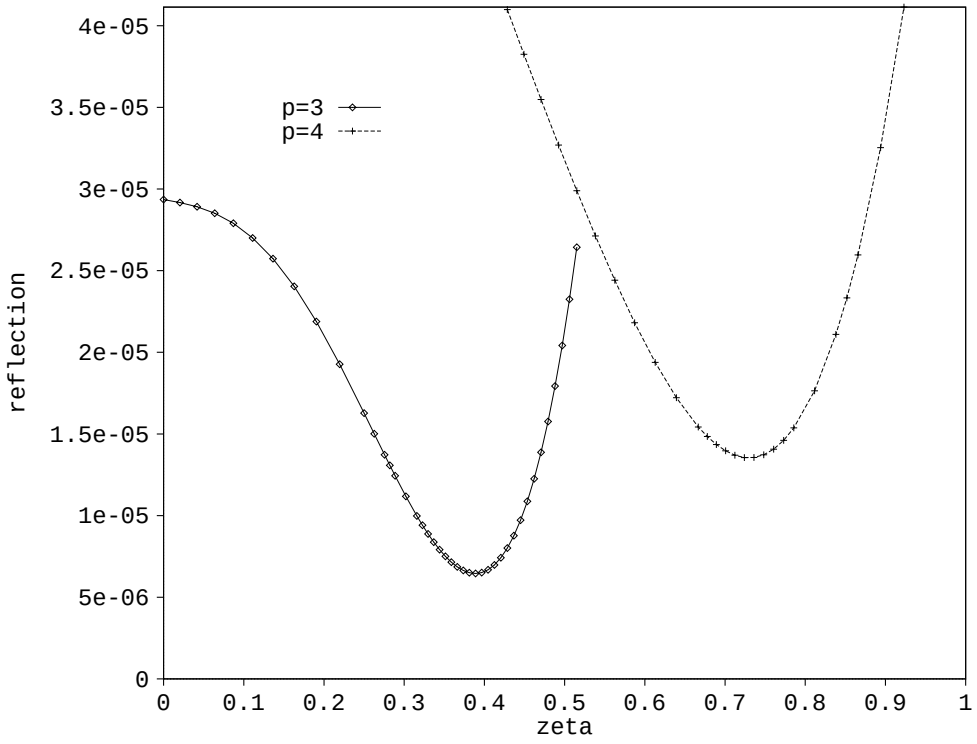


FIG. 4.9. *Reflection ratio as a function of* $\zeta$ *for* $K_0 = 15.0$ *at* $t = 0.3$.

distributed about $\hbar K_0/m$. Thus, if we use the same double Gaussian distribution calculation as before but vary the group velocities of the absorbing boundary condition for $p = 4$,

$$a_1 = \frac{\hbar K_0}{m}, \quad a_2 = (1+\zeta)\frac{\hbar K_0}{m}, \quad a_3 = \frac{\hbar K_1}{m}, \quad a_4 = (1+\zeta)\frac{\hbar K_1}{m}, \tag{4.17}$$

where $\zeta$ is the variation of group velocity, then we obtain the results shown in Figure 4.11. We again can see that when $a_2$ and $a_4$ are increased, the reflection properties of the $p = 4$ absorbing boundary condition were improved to a peak absorption near $\zeta = 1.8$. Hence, the more spread out the interpolation points of the dispersion relation, the better the performance of the absorbing boundary condition for this initial double Gaussian distribution.

**4.3.4. Narrow Gaussian pulse distribution.** We would also like to consider the effect of narrowing the spatial spread of the initial Gaussian distribution and thus having a wider distribution of momentum in momentum space [6]. In particular, we would like to consider the effect of this modification on the relative reflective properties of the $p = 3$ and $p = 4$ absorbing boundary conditions. Therefore, we will use a narrow Gaussian pulse in the form of a Gaussian distribution (4.14) with $L = 10, \sigma_0 = L/100$, and $\xi = 3L/4$. Note that this distribution is one-tenth as wide as the previous Gaussian distributions. As the $\sigma_0$ approaches zero, Gaussian pulse narrows. Again, $\delta = 0.0001$ and $\epsilon = L/512$, as before.

We performed calculations (i) with no absorbing boundary condition present (i.e.,

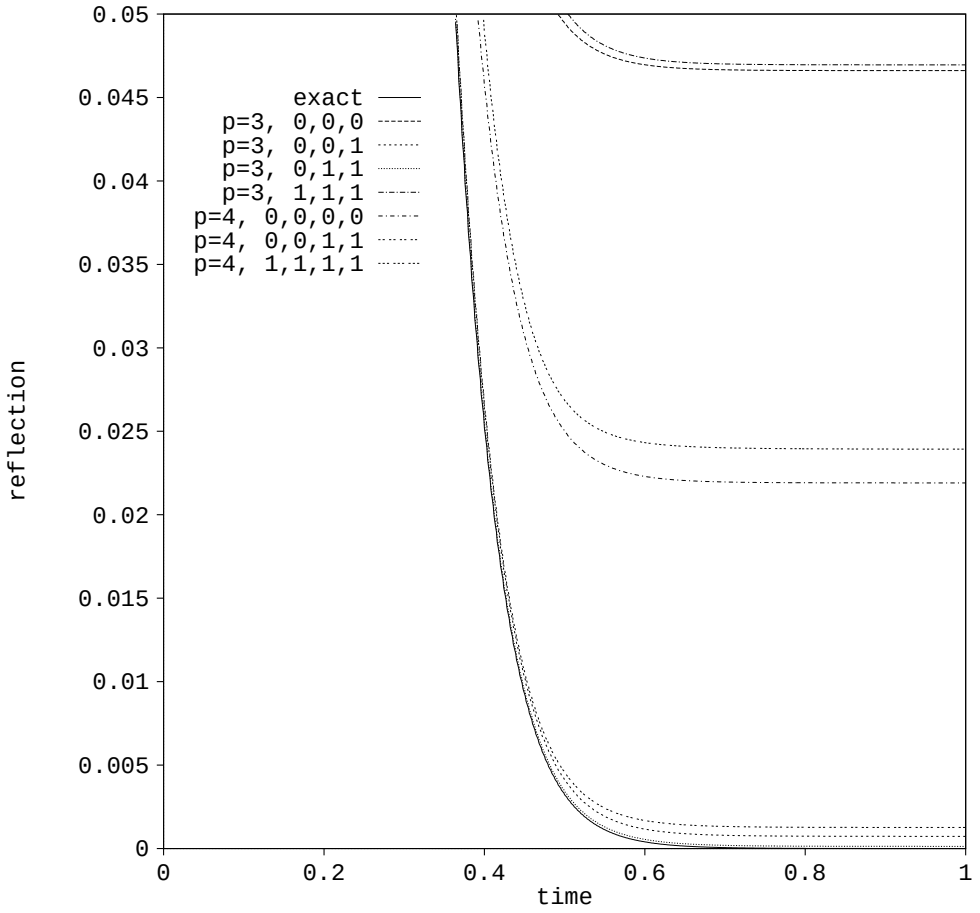


FIG. 4.10. *Reflection ratio as a function of time for double Gaussian with* $K_0 = 25.0$ *and* $K_1 = 5.0$.

the ideal boundary condition), (ii) with a $p = 3$ absorbing boundary condition with $a_i = \hbar K_0/m$, and (iii) with a $p = 4$ absorbing boundary condition with $a_i = \hbar K_0/m$. At $t = 1$ ($n = 10,000$), these simulations have $r$ values of $2.5959 \times 10^{-2}, 3.1246 \times 10^{-2}$, and $2.866 \times 10^{-2}$, respectively. Therefore, with the narrower initial spread but wider distribution in momentum space, the $p = 4$ absorbing boundary condition is more effective.

If we use the same narrow Gaussian pulse distribution calculation but vary the group velocities of the absorbing boundary condition for $p = 4$—$a_1 = a_2 = a_3 = a_4 = (1 + \zeta)\frac{\hbar K_0}{m}$, where $\zeta$ is the variation of group velocity—then we obtain the results in Figure 4.12. The properties displayed in this figure are different from those for the Gaussian with wider initial spreads, $\sigma_0$. Since the narrow Gaussian pulse spreads so quickly as a function of time when evolved by the Schrödinger equation, it turns out that decreased values of $a_i$ lead to a minimized reflection ratio, whereas for the wider initial distributions, the larger values of $a_i$ were more effective.

**5. Discussion.** For the three types of initial distribution simulations, we find that the higher the order of the absorbing boundary condition, the better the reflection

TABLE 4.2
*Comparison of reflection ratios vs. different schemes for double Gaussian distribution.*

| *No.* | *Scheme* | $a_1$ | $a_2$ | $a_3$ | $a_4$ | *time* | $r$ |
|---|---|---|---|---|---|---|---|
| 1 | Exact implicit | $---$ | $---$ | $---$ | $---$ | 0.84 | $5.111 \times 10^{-6}$ |
| 2 | $p = 3$ implicit | $\frac{\hbar K_0}{m}$ | $\frac{\hbar K_0}{m}$ | $\frac{\hbar K_0}{m}$ | $---$ | 0.84 | $4.661 \times 10^{-2}$ |
| 3 | $p = 3$ implicit | $\frac{\hbar K_0}{m}$ | $\frac{\hbar K_0}{m}$ | $\frac{\hbar K_1}{m}$ | $---$ | 0.84 | $7.364 \times 10^{-4}$ |
| 4 | $p = 3$ implicit | $\frac{\hbar K_0}{m}$ | $\frac{\hbar K_1}{m}$ | $\frac{\hbar K_1}{m}$ | $---$ | 0.84 | $1.368 \times 10^{-4}$ |
| 5 | $p = 3$ implicit | $\frac{\hbar K_1}{m}$ | $\frac{\hbar K_1}{m}$ | $\frac{\hbar K_1}{m}$ | $---$ | 0.84 | $4.696 \times 10^{-2}$ |
| 6 | $p = 4$ implicit | $\frac{\hbar K_0}{m}$ | $\frac{\hbar K_0}{m}$ | $\frac{\hbar K_0}{m}$ | $\frac{\hbar K_0}{m}$ | 0.84 | $2.191 \times 10^{-2}$ |
| 7 | $p = 4$ implicit | $\frac{\hbar K_0}{m}$ | $\frac{\hbar K_0}{m}$ | $\frac{\hbar K_0}{m}$ | $\frac{\hbar K_1}{m}$ | 0.84 | $3.295 \times 10^{-3}$ |
| 8 | $p = 4$ implicit | $\frac{\hbar K_0}{m}$ | $\frac{\hbar K_0}{m}$ | $\frac{\hbar K_1}{m}$ | $\frac{\hbar K_1}{m}$ | 0.84 | $1.270 \times 10^{-3}$ |
| 9 | $p = 4$ implicit | $\frac{\hbar K_0}{m}$ | $\frac{\hbar K_1}{m}$ | $\frac{\hbar K_1}{m}$ | $\frac{\hbar K_1}{m}$ | 0.84 | $8.468 \times 10^{-4}$ |
| 10 | $p = 4$ implicit | $\frac{\hbar K_1}{m}$ | $\frac{\hbar K_1}{m}$ | $\frac{\hbar K_1}{m}$ | $\frac{\hbar K_1}{m}$ | 0.84 | $2.394 \times 10^{-2}$ |

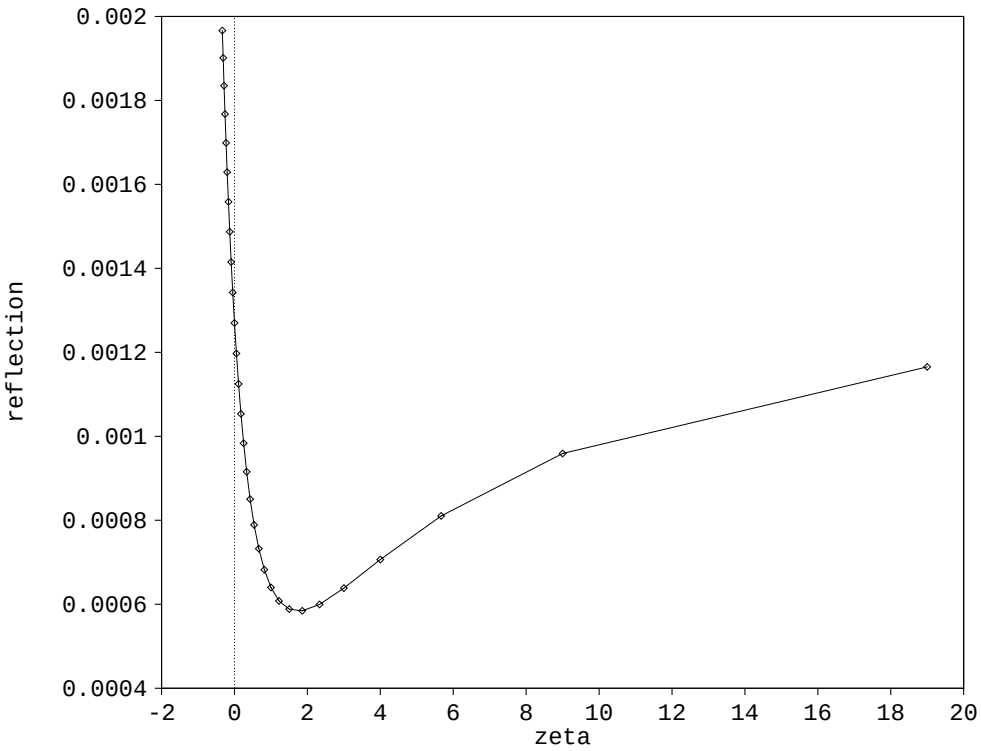


FIG. 4.11. *Reflection ratio as a function of* $\zeta$ *at* $n = 8400$ $(t = 0.84)$ *for double Gaussian distribution with* $p = 4$ *absorbing boundary condition.*

ratio properties (ignoring the essentially equivalent behavior of the $p = 3$ and $p = 4$ absorbing boundary conditions for a moment). The Dirichlet boundary condition, on the other hand, produced total reflection of the incident wave. This was not surprising, since the $\Psi = 0$ would have appeared to the wave as a wall of infinite potential value which was impossible to overcome, and thus the wave was completely reflected.

For the single Gaussian distribution, with the momentum being strongly peaked around a single $K_0$ value, the effectiveness of the $p = 3$ and $p = 4$ absorbing bound-

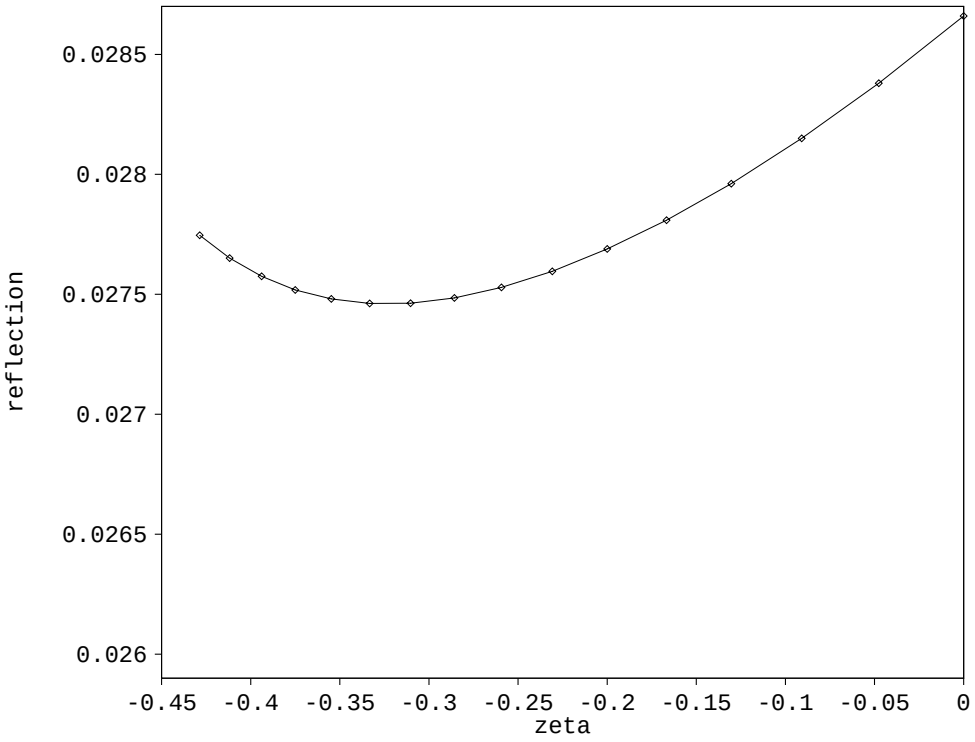


FIG. 4.12. *Reflection ratio as a function of* $\zeta$ *at* $n = 8400$ $(t = 0.84)$ *for narrow Gaussian pulse with a* $p = 4$ *absorbing boundary condition.*

ary conditions was roughly equivalent. The fact that the $p = 4$ absorbing boundary condition was not more effective for strongly peaked momentum distributions than the $p = 3$ absorbing boundary condition was contrary to our expectations from the reflection ratio value as predicted by (3.20).

The greater accuracy for the $p = 3$ absorbing boundary condition can be understood in the following sense. In general, the accuracy of an absorbing boundary condition depends on how accurately the interpolation of the dispersion relation models the exact dispersion relation. Hence, for distributions with wide distributions in momentum space, such as for the narrow Gaussian pulse, the $p = 4$ absorbing boundary condition is more effective, similar to when there are two or more distinct peaks in the momentum distribution. But when there is only a small distribution in momentum space around the single interpolation point in the dispersion relation, other factors are important. First, the accuracy of the absorbing boundary condition is limited by the consistency error associated with the discretization of the differential operators. Since this error is roughly equivalent for the $p = 3$ and $p = 4$ absorbing boundary conditions, there must also be another factor. This factor stems from the fact that the absorbing boundary condition admits a generalized eigenvalue with zero group velocity on the boundary, as shown previously. We conjecture that the higher order absorbing boundary condition may cause this generalized eigenvalue to admit more error, hence causing the $p = 4$ absorbing boundary condition to be less effective. A similar effect was observed by Higdon for his general absorbing boundary condition for the wave equation. He states that "the generalized eigenvalue can cause mild instabilities con-

sisting of waves radiating spontaneously into the interior of the boundary" [9]. This behavior does not seem to affect the overall stability properties of the $p = 4$ absorbing boundary condition, as the error did not grow unboundedly with time. Therefore, for waves which have small momentum spreads about a peak momentum value, the $p = 3$ absorbing boundary condition might be expected to be more effective, whereas for waves with large momentum spreads, the $p = 4$ absorbing boundary condition might be expected to be more effective and the error caused by the generalized eigenvalue is less prevalent. Of course, varying the adjustable parameters usually improves the behavior of either.

All the absorbing boundary conditions were more effective at lower values of $K_0$ (for the range of $K_0$ presented here), as can be seen in Table 4.1, contrary to the results presented in Kuska's paper [19], whose minimum reflection value appears for $K_0 \approx 15$. Of course, as the values $K_0$ tend to zero, the dispersion relation has a steeper gradient, and thus the approximations for a fixed order become less accurate. Accordingly, the behavior of the absorbing boundary conditions will become poorer.

Kuska's results for identical calculations are different from those presented in this paper due to the nature of the cutoff criterion that Kuska [19] used to compare various values of $K_0$, where the simulations were terminated when the relation $(\sum_{j=0}^{\mathcal{J}} x|\Psi_j^n|^2)/(\sum_{j=0}^{\mathcal{J}} |\Psi_j^0|^2) < \hat{\epsilon}$ is satisfied. Kuska does not discuss how the value $\hat{\epsilon}$ is determined. Regardless, this cutoff criterion will be insensitive to peculiarities in the behavior of different waves and it does not account for multiple reflections off different boundaries, whereas our plateau comparison method does. This is particularly a problem for lower energy waves in a small domain because the reflected wave will impinge on the opposite boundary before the incident wave has passed completely through the first boundary. Furthermore, due to the nature of Kuska's cutoff criterion, the values of $r$ which Kuska presents are orders of magnitude higher than those presented here, for equivalent schemes. (For example, the lowest value for a reflection ratio which Kuska presents is $1.0 \times 10^{-3}$.) This is due to the choice of a relatively large value of $\hat{\epsilon}$ to accommodate a large range of energies.

Figure 4.9 shows that the $p = 3$ absorbing boundary condition was more effective for different ranges in momentum space than the $p = 4$ absorbing boundary condition. The $p = 4$ absorbing boundary condition was more effective with larger group velocity values for the parameters of the absorbing boundary condition. These results are related to the forms of the interpolation forms for the absorbing boundary conditions relative to the exact dispersion relation and the evolving group velocity characteristics of the Gaussian distributions.

For the narrow Gaussian pulse, the Gaussian distribution is more sharply peaked, but in momentum space the momentum distribution is broader. Therefore, when evolved by the Schrödinger equation, the different momentum components cause the distribution to flatten quickly, since the components will be traveling at different velocities. In this case, the $p = 4$ absorbing boundary condition fared better than the $p = 3$ absorbing boundary condition. Thus it can be concluded that the $p = 4$ absorbing boundary condition was effective in reducing the amplitude of components of a wider range of momentum values about a peak value than was the $p = 3$ absorbing boundary condition, as discussed above.

But the real power of the general absorbing boundary condition is expressed when used in conjunction with multiple Gaussian distribution with different momentum peaks. This is a more realistic test, since in a practical application more than one value of $K_0$ would be expected to be present. Our results are primarily presented by Figure

4.10. Here the claim that the $p = 4$ absorbing boundary condition is more effective for a wider distribution of momentum values is further illustrated for the simulations using $a_i = a_j, i \neq j$ for the absorbing boundary conditions. This can be understood from the fourth order interpolation being a better approximation to the dispersion relation over a wider range of momentum around $\hbar K_0$ in the dispersion relation. Also, when the flexibility of the absorbing boundary conditions is exploited, such as when the interpolations points are tuned to the two distinct peaks of momentum, $\hbar K_0$ and $\hbar K_1$, the amount of reflection produced by the absorbing boundary conditions is considerably reduced. Whereas the minimum reflection that an absorbing boundary condition based on Kuska's homogeneous absorbing boundary condition (3.5) could produce is $4.66 \times 10^{-2}$, when the parameters for the $p = 3$ absorbing boundary condition are tuned to both peaks the reflection ratio falls to $1.37 \times 10^{-4}$, a reduction of more than two orders of magnitude. Interestingly, when tuned to the momentum peaks, the $p = 3$ absorbing boundary condition again proved more effective than the $p = 4$ absorbing boundary condition (again probably due to the mild instability associated with the generalized eigenvalue), although the latter allows for one more adjustable parameter which could be useful for even more general incident waves.

To summarize, the absorbing boundary conditions are effective choices for boundary conditions where the boundary must not interfere with the interior solution, unlike the standard Dirichlet boundary condition. The general absorbing boundary condition developed in this paper is flexible enough to be adapted for a wide range of incident waves, either with multiple group velocities or with wide distributions in momentum space, while producing a minimal amount of reflection.

## REFERENCES


[1] A. Bayliss and E. Turkel, *Radiation boundary conditions for wave-like equations*, Comm. Pure Appl. Math, 33 (1980), pp. 707–725.

[2] B. Engquist and A. Majda, *Absorbing boundary conditions for the numerical simulation of waves*, Math. Comp., 31 (1977), pp. 629–651.

[3] B. Engquist and A. Majda, *Radiation boundary conditions for acoustic and elastic wave calculations*, Comm. Pure Appl. Math., 32 (1979), p. 314–358.

[4] T. Fevens and H. Jiang, *Absorbing boundary conditions for the Schrödinger equation*, Technical Report 95-376, Department of Computing and Information Science, Queen's University, Kingston, Ontario, Canada, 1995.

[5] I. Galbraith, Y. S. Ching, and E. Abraham, *Two-dimensional time dependent quantum-mechanical scattering event*, Amer. J. Phys., 52 (1984), pp. 60–68.

[6] A. Goldberg, H. M. Schey, and J. L. Schwartz, *Computer-generated motion pictures of one-dimensional quantum-mechanical transmission and reflection phenomena*, Amer. J. Phys., 35 (1967), pp. 177–186.

[7] B. Gustafsson, H.-O. Kreiss, and A. Sundström, Math. Comput., 26 (1972), p. 649.

[8] C. A. Hall and T. A. Porsching, *Numerical Analysis of Partial Differential Equations*, Prentice–Hall, Englewood Cliffs, NJ, 1990.

[9] R. L. Higdon, *Absorbing boundary conditions for difference approximations to the multi-dimensional wave equation*, Math. Comp., 47 (1986), pp. 437–459.

[10] R. L. Higdon, *Initial-boundary value problems for linear hyperbolic systems*, SIAM Rev., 28 (1986), pp. 177–217.

[11] R. L. Higdon, *Numerical absorbing boundary conditions for the wave equation*, Math. Comp., 49 (1987), pp. 65–90.

[12] R. L. Higdon, *Radiation boundary conditions for elastic wave propagation*, SIAM J. Numer. Anal., 27 (1990), pp. 831–869.

[13] R. L. Higdon, *Radiation boundary conditions for dispersive waves*, SIAM J. Numer. Anal., 31 (1994), pp. 64–100.

[14] H. Jiang and Y. S. Wong, *Absorbing boundary conditions for second-order hyperbolic equations*, J. Comput. Phys., 88 (1990), pp. 205–231.

[15] R. Keys, *Absorbing boundary conditions for acoustic media*, Geophy., 50 (1985), pp. 892–902.
[16] R. Kosloff and D. Kosloff, *Absorbing boundaries for wave propagation problems*, J. Comput. Phys., 63 (1986), pp. 363–376.
[17] H.-O. Kreiss, *Initial boundary value problems for hyperbolic systems*, Comm. Pure Appl. Math., 23 (1970), pp. 277–298.
[18] H.-O. Kreiss and J. Lorenz, *Initial-Boundary Value Problems and the Navier-Stokes Equations*, Academic Press, Boston, 1989.
[19] J.-P. Kuska, *Absorbing boundary conditions for the Schrödinger equation on finite intervals*, Phys. Rev. B, 46 (1992), pp. 5000–5003.
[20] D. Neuhauser and M. Baer, *The time-dependent Schrödinger equation: Application of absorbing boundary conditions*, J. Chemical Phys., 90 (1989), pp. 4351–4355.
[21] R. Renaut, *Absorbing boundary conditions, difference operators, and stability*, J. Comput. Phys., 102 (1992), pp. 236–251.
[22] R. Sakamoto, *Hyperbolic Boundary Value Problems*, Cambridge University Press, New York, 1982.
[23] T. Shibata, *Absorbing boundary conditions for the finite-difference time-domain calculation of the one-dimensional Schrödinger equation*, Phys. Rev. B, 43 (1991), pp. 6760–6763.
[24] L. N. Trefethen, *Group velocity in finite difference schemes*, SIAM Rev., 24 (1982), pp. 113–136.
[25] L. N. Trefethen, *Group velocity interpretation of the stability theory of Gustafsson, Kreiss and Sundström*, J. Comput. Phys., 49 (1983), pp. 199–217.
[26] L. N. Trefethen and L. Halpern, *Well-posedness of one-way wave equations and absorbing boundary conditions*, Math. Comp., 47 (1986), pp. 421–435.